Energy Proceedings
Vol 53, 2025
ISSN 2004-2965

# Reduce graphene oxide modified porous carbon foam as anode electrode for increased performance of a non-aqueous thermally regenerative battery#

Yichao An[1,2], Zhenchong Xiao[1,2], Liulin Que[1,2], Liang Zhang[1,2*], Jun Li[1,2], Xun Zhu[1,2], Qiang Liao[1,2]
1 Key Laboratory of Low-grade Energy Utilization Technologies and Systems, Chongqing University, Ministry of Education, Chongqing, 400030, China
2 Institute of Engineering Thermophysics, School of Energy and Power Engineering, Chongqing University, Chongqing, 400030, China
(Liang Zhang: liangzhang@cqu.edu.cn)

**ABSTRACT**

Non-aqueous thermally regenerative batteries (NTRBs) hold significant potential for efficiently converting low-grade waste heat into electricity, offering broad application possibilities. Nevertheless, the specific surface area of the reported electrodes restricted both the electrochemical reaction rate and electricity generation. In this work, the reduced graphene oxide modified porous carbon foam(rGO/CF) was proposed to serve as an anode electrode for NTRB to promote the electricity generation of NTRB. The maximum power density of the NTRB with rGO/CF electrodes reached its peak at 190.2 W/m², showing enhancements of 15% compared to carbon foam. The enhanced performance was primarily attributed to the abundant active sites, large specific surface area, and favorable porous electrode structure. Moreover, the stability of the rGO/CF electrodes was confirmed with a continuous operation exceeding 270 minutes and enduring through more than 8 cycles. In conclusion, NTRB-rGO/CF showed great promise for applications in converting low-grade waste heat into electricity.

**Keywords:** non-aqueous thermally regenerative battery, reduced graphene oxide, waste heat recovery, maximum power density.

**NONMENCLATURE**

| | |
|---|---|
| *Abbreviations* | |
| NTRB | The non-aqueous thermally flow regenerative battery |
| RVC | Reticulated vitreous carbon |
| CF | Porous Carbon Foam |
| GO/CF | Graphene oxide modified porous carbon foam |
| rGO/CF | Reduced graphene oxide modified porous carbon foam |
| *Symbols* | |
| $I$ | Current |
| $U$ | Voltage |
| $P_s$ | Power density |
| $\eta$ | Thermal efficiency |

## 1. INTRODUCTION

Approximately 20-50% of the energy generated in industrial production was released into the environment as low-temperature waste heat. This phenomenon not only results in significant resource wastage but also contributes to environmental pollution [1]. Converting low-grade waste heat into electricity could not only bring both economic and environmental benefits but also significantly reduce environmental pollution [2, 3]. Currently, common liquid-based thermoelectric conversion technologies include thermo-electrochemical cell (TEC) [4, 5], thermally regenerative electrochemical cycle (TREC) [6, 7], thermally regenerative battery (TRB)[8-10], and direct thermal charge cell (DTCC) [11, 12]. Among them, TRBs had broader application prospects due to the mild reaction conditions, low cost, and excellent electricity generation [13].

In the conventional TRBs, the low-grade waste heat was utilized to break the complexation of copper-ammonia complexes in the anode-exhausted electrolyte, which would generate active substances (ammonia) and catholyte. The exhausted catholyte could serve as the anolyte for the next cycle, thus enabling thermally regenerative batteries to achieve multi-batch cyclic power generation [14]. In the power generation process of TRBs, the anodic reaction was the reaction between metallic copper and ammonia, and the cathodic reaction was the deposition of cupric ions. It should be noted that the multi-batch cyclic power generation for recovering low-grade waste heat could only be realized by exchanging the cathode and anode electrodes. To

# This is a paper for the 16th International Conference on Applied Energy (ICAE2024), Sep. 1-5, 2024, Niigata, Japan.

improve the electricity generation of TRBs, copper foam was proposed to replace the copper sheet, which improved the specific surface area of the electrodes and enhanced the electrochemical reactions [15]. However, the corrosive effect of ammonia on the anode electrodes restricts electron conduction, resulting in a low anode coulombic efficiency [16, 17]. At the same time, the side reactions [18] in the catholyte would lead to a continuous loss of the electrodes, which severely limited the electricity generation and the cycling stability. Furthermore, the high latent heat of vaporization of water absorbed a significant amount of heat, posing challenges to the recycling of anode waste liquid in thermally regenerative batteries [19]. Therefore, the non-aqueous thermally regenerative batteries (NTRB) based on the electrochemical reactions between the acetonitrile and nano copper were proposed [20]. The anodic electrochemical reaction was the conversion of nano copper to cuprous ions, and the cathodic electrochemical reaction was the conversion of cupric ions to cuprous ions, as follows.

Cathodic reaction:

$$Cu(CH_3CN)_4^{2+} + e^- \rightarrow Cu(CH_3CN)_2^+$$

Anodic reaction:

$$Cu(s) \rightarrow Cu^+ + e^-$$

Thermal regeneration：

$$2Cu(CH_3CN)_4^+ \xrightarrow{\Delta} Cu(s) + Cu^{2+} + 8CH_3CN$$

This not only prevented corrosion of the anode electrode during electricity production but also enhanced the anode coulomb efficiency, thereby further improving resource utilization. Additionally, the electricity generation and thermoelectric conversion efficiency of NTRBs exceeded that of traditional TRBs [21], highlighting their promising potential for converting low-temperature waste heat.

Considering the limited electrochemical reactions and the solid-liquid two-phase flow of anolyte, the optimal structure of the anode electrodes mattered a lot. In previous work, the reticulated vitreous carbon (RVC)anode has low electrochemical performance because of the small specific surface area, which constrained the power generation performance. Therefore, a reduced graphene oxide modified porous carbon-based composite electrode (rGO/CF) was developed in this work. The reduced graphene oxide (rGO) was known for its abundant defects and pore structure, which was suitable for this situation. The modification of rGO was to increase the electrode's specific surface area and reduce the flow resistance of the anolyte, thereby enhancing battery performance. To obtain adjustable pores of the electrodes, the polyurethane foam was synthesized in a single step and used as a substrate, which was impregnated with resin and carbonized at high temperatures to form a porous carbon material. Subsequently, reduced graphene oxide was incorporated into the porous carbon material to create the composite electrode material. It was expected that the rGO/CF would enhance the electricity generation of NTRBs for the reasonable pore distribution and more active sites, which would reduce the resistance of mass transfer and improve the electricity generation of NTRBs.

## 2. MATERIAL AND METHODS

### *2.1 The preparation of the electrode*

The porous carbon material was prepared by the template method, and the porous composite electrode was obtained by modifying reduced graphene oxide on the carbon material. The specific preparation process of the CF/rGO composite electrode was shown in Fig.1, which was mainly divided into two parts. In the first part, flexible polyurethane foam was synthesized by a one-step method [22]. Water, silicone oil (≥99.0 %, Shanghai Titan Technology Co., Ltd.), dibutyl tin dilaurate (95 %, Shanghai Titan Technology Co., Ltd.), and triethanolamine (97 %, Chengdu Colony Ltd.), mixed homogeneously and heated to 60 ℃. Toluene diisocyanate (TDI) was then added to the mixture and the mixture was stirred at a stirring rate of 1200 rpm to allow free foaming of the polyurethane foam. The polyurethane foam was washed with ethanol and water to remove unreacted impurities from the surface and dried in an oven at 60 °C. The dried polyurethane foam was immersed in 70 mL of acetone (99.5%, Shanghai Taitan Technology Co., Ltd.) solution with 1 g of p-toluene sulfonic acid (98%, Shanghai Taitan Technology Co., Ltd.) dissolved in it for 10 min, and then dried in an oven at 100 ℃ for 1 h. The acetone was completely volatilized, and the p-toluene sulfonic acid was adhered to the polyurethane surface. A certain amount of furfuryl alcohol was dripped into the dried polyurethane foam so that the furfuryl alcohol was uniformly coated on the surface of the polyurethane foam, and then the reaction was carried out in an oven at 100 ℃ for 2 h. The furfuryl alcohol was catalyzed by p-toluene sulfonic acid on the surface of the foam, and then it was changed into furan resin so that the surface-loaded furan resin was obtained as the carbonized precursor. The carbonized precursor was transferred to a tube furnace and heated at a temperature of 950 ℃ for 2 h with a heating rate of 2 ℃/min. Finally, the carbonized carbon material was

thoroughly rinsed with deionized water and anhydrous ethanol and dried in an oven at 80 ℃ for 8 h, and the porous carbon material was obtained.

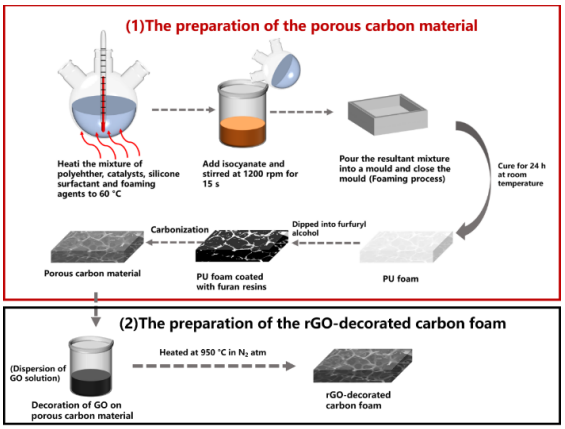


*Fig. 1* Scheme of the preparation of the rGO/CF composite electrode

The prepared porous carbon material was put into a certain concentration of Graphene Oxide (GO) (20-30 μm, Shanghai Titan Technology Co., Ltd.) dispersion, and immersed for 1 h. After removal, it was dried naturally in the air to remove excess water, and then the dried porous carbon samples were put into the graphene oxide dispersion again for 1 h, followed by drying in an oven at 50 ℃. The process was repeated 3 times. Subsequently, the graphene oxide/porous carbon samples were transferred to a tube furnace and heated at 950 ℃ for 2 h under a nitrogen atmosphere, and the reduction reaction of graphene oxide occurred at high temperatures. Finally, the carbon foam modified by reduced graphene oxide (rGO) was obtained.

### *2.2 The construction and operation of TRFB*

Anode and cathode collector size is 50×50 mm, 10 mm thick, titanium metal surface gold plated material, each collector side has a size of 20×10×2 mm electrode chamber for the cathode/anode electrode. The anode and cathode chamber are separated by an anion exchange membrane (AEM), and a 1 mm thick silicone gasket of the same size is placed between the membrane and the chamber to seal the device and prevent electrolyte leakage. The titanium baffle is 80×50mm in size and 2 mm thick and is used to export electrons for relevant electrochemical tests. The anode and cathode partitions are 80×80×10mm in size and made of ABS resin, which are placed at both ends to fix the entire reactor structure. The reactor was fixed with 4 bolts from top to bottom and left to right for the copper nanoflow battery experiment. At the same time, the complete experimental equipment also includes a storage tank for storing the electrolyte, a silicone hose for conveying the electrolyte, and a peristaltic pump to drive the electrolyte to the reactor chamber, with a flow rate of 30 to 40 mL/min. In this experiment, the concentration of copper ion in the cathode of NTRB using composite electrode is 0.1 mol/L, the concentration of supporting electrolyte is 0.15 mol/L, the volume fraction of acetonitrile is 50%, the mass fraction of copper particles in the anodic solution is 15%, the cathode electrode is KOH etching electrode (ECF), and the liquid flow reactor is used in this section. The same experimental conditions were applied to porous carbon material (Carbon foam (CF)) prepared by polyurethane template, and composite electrode (CF/rGO) modified with rGO. The preparation parameters of porous carbon materials were foam stabilizer content 100:7, furfuryl alcohol content 0.4 mL, and graphene oxide concentration 1 mg/mL.

### *2.2 Material and Methods*

Scanning electron microscopy (3400 N, HITACHI instrument) and Energy Dispersive Spectroscopy (EDS, Apollo XLT SDD, EDAX) were used to observe and analyze the microscopic morphology of the electrodes, which provided visual pore distribution on the electrode surface. The mercury intrusion porosimeter (MIP) was used to analyze the distribution of the pore size and the specific surface area of the electrode. The polarization experiments of the battery were performed by linear sweep voltammetry (LSV) with an electrochemical workstation (Princeton). The scanning voltage range was set according to the open circuit voltage of the battery, and the scanning rate was 10 mV/s. The scan frequency of the Electrochemical Impedance Spectroscopy (EIS) test is 100 kHz to 0.1 Hz, and the sinusoidal amplitude is 10 mV.

### *2.3 Theory/calculation*

The output power density of the battery was $P_s = UI/S$, where $S$ was the projected electrode area of the three-dimensional porous electrode, $1\times10^{-4}$ $m^2$. The current density was calculated as

$$I_s = I/S \quad (1)$$

The discharging current of the battery was 10 mA, and the actual energy density of TRFB was calculated by

$$E = \int UIdt/V \quad (2)$$

where $V$ was the volume of the electrolytes.

Theoretical thermal regeneration efficiency $\eta$ is calculated by the following formula:

$$\eta = \frac{W_{elec}}{2Q} = \frac{nFE_{cell}c}{2(Q_1 + Q_2 + Q_3)} = \frac{nFE_{cell}c}{2(\Delta H_{vap}^{ACN} \times c_{ACN} + \Delta T \times C_p \times c_{sol} + \Delta H_{rxn}^{Cu\ /} \times c_{[Cu(ACN)4}} \quad (3)$$

Q is the heat absorbed in the thermal regeneration process of the electrolyte per unit volume (kJ/L), $W_{elec}$ is the theoretical energy density of the battery (kJ/L), and the coefficient 2 in the denominator is because both the anode and cathode electrolyte need to be regenerated. $Q_1$ is the latent heat of vaporization of acetonitrile evaporation; $Q_2$ is the heat absorbed by the temperature rise of acetonitrile and propylene glycol carbonate ester cosolvent; $Q_3$ is the heat absorbed by the decomposition of cuprous acetonitrile complex. n is the number of electrons transferred in the electrochemical reaction; F is the Faraday constant (F=96485 C/mol); $E_{cell}$ is the open circuit voltage of the non-aqueous thermal regenerative battery (V); $c_{[Cu(ACN)4]+}$c is the concentration of copper ions in the cathode electrolyte (mol/L).

## 3. RESULTS AND DISCUSSION

### *3.1 The verification of rGO/CF*

The change of composite carbon electrode microscopy in the preparation process was observed using SEM and EDS. The results were shown in Fig.2. After polyurethane foam carbonization, the skeleton shrinked and the pore became larger. As for, the carbon skeleton was intact without fracture, providing a stable skeleton for rGO. Additionally, the loading of GO was confirmed through Energy Dispersive Spectroscopy (EDS) analysis of the oxygen distribution in GO/CF. The oxygen content on the electrode surface was found to be 13.79% with a uniform distribution. The uniform load of graphene oxide was expected to provide the electrode with a higher specific surface area. Considering the specific solid-liquid two-phase flow of anolyte, the big pores served as mass transfer channels in anolyte was necessary. The modification of rGO was expected to provide more small pores, which would increase the specific surface area without limiting mass transfer, which would help enhance the electricity generation of NTRBs.

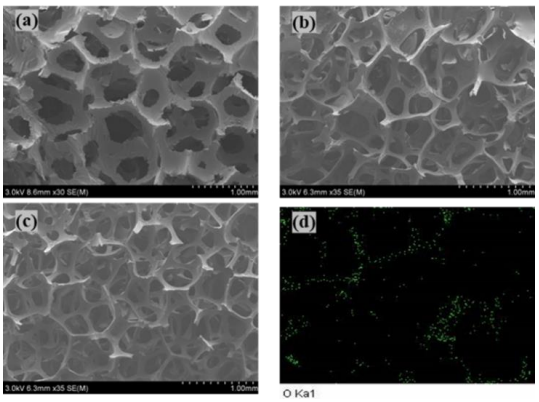


Fig.2 SEM images of polyurethane foam (a), carbonized foam material (b) composite electrode(c), and EDS of GO/CF composite electrode (d).

Furthermore, the XRD and Raman spectroscopy was carried out to further determine the preparation of rGO/CF and the defect levels of the different electrodes. The diffraction peak of GO/CF at 11.2 ° was consistent with the diffraction peak of GO [23] (001), which indicates that GO was successfully loaded on the CF. After the reduction in high temperature, the characteristic peak disappeared, which proved that the GO was fully reduced to rGO. Notably, the ID/IG value of rGO/CF is 1.20, higher than GO/CF (1.00) and CF (1.03) The ID/IG, which was due to the removal of GO oxygen-containing groups accompanied by more defects [24]which would provide more active sites for electrochemical reactions and thus hopefully improve the electricity generation of NTRBs.

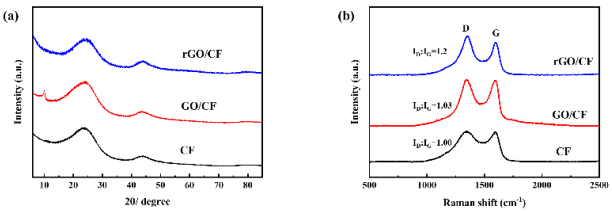


Fig.3 XRD patterns(a) and Raman spectrums(b) of CF, GO/CF, and rGO/CF.

### *3.2 The specific surface area of different electrodes*

The porous structure and many defects of rGO/CF demonstrated its potential as an electrode for NTRBs. To further explore its advantages, the pore distribution and specific area of CF and rGO/CF were analyzed. After the modification of rGO, the specific surface area was increased to 158.5 $m^2/g$, which was increased by 16.8 times. The increase in surface area was mainly due to the increase of the small pores. Moreover, the increase of specific areas was expected to provide a more adequate active site for the electrochemically active area, thus

hopefully enhancing the electricity generation. In addition, the average pore size of both CF and rGO/CF was approximately equal, which would not restrict the mass transfer of the nano-fluid flow in anolyte. It was presumed that the higher specific surface area would provide more active sites for electrochemical reactions without increasing the mass transfer resistance, thus improving the electricity generation of NTRBs.

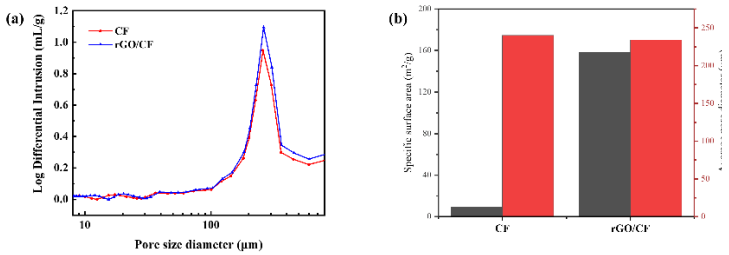


Fig.4 Distribution of pore diameter of CF and composite electrode (CF/rGO).

### *3.3 The electricity generation with different electrodes*

To investigate the influence of different electrodes on the electricity generation of NTRB, the linear voltammetry and electrochemical impedance of CF and rGO/CF electrodes were carried out, as shown in Fig.5. The maximum power density of NTRB-rGO/CF reached to 190.2 W/m², which represents a 15% increase compared to NTRB-CF. This was due to the high specific surface area, more defects, and more reaction sites of rGO/CF, which would strengthen the charge transfer at the electrode interface. At the same time, the average pore size of rGO/CF was similar to CF, which guaranteed the transmission of reactants in the electrode. In addition, the ohmic internal resistance of NTRB-CF and NTRB-CF/rGO was almost equal (5.5 Ω), which revealed that the conductivity of the electrodes would not be affected by the modification of rGO. Furthermore, after the modification of rGO, charge transfer impedance was reduced to 17.3 Ω and mass transfer impedance was decreased to 4.0 Ω. This was mainly because rGO/CF provided large channels for mass transfer and more active sites for electrochemical reactions, which not only enhanced the charge transfer of the electrode but also facilitated the transmission of the reactants inside the electrode. In summary, because of the large specific area, the rich defects and the large channel for mass transfer of rGO/CF, the maximum power density reached its peak at 190.2 W/m².

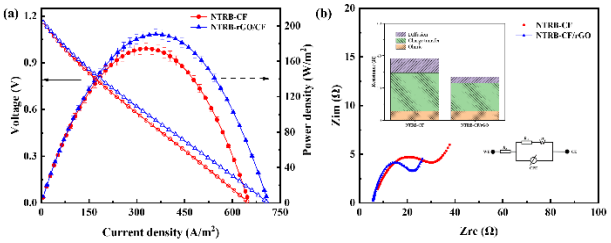


Fig.5 Electricity generation performance(a) and Nyquist plots (b)of NTRB-CF and NTRB-CF/rGO.

### *3.4 The stability of the electricity generation*

The stability of power generation cycling was another key factor in judging the application potential of the electrodes [25]. To verify the stability of the rGO/CF, constant current charge/discharge (Galvanostatic charge/discharge (GCD)) tests were carried out on NTRB-CF/rGO. The charge/discharge test was performed at a constant current of 10 mA with a discharge cutoff voltage of 0.7 V and a charge process cutoff voltage of 1.45 V. The results were shown in Fig. 6a. The rGO/CF exhibited good stability, maintaining stable cycling performance for more than 8 batches (270 minutes). That showed the possible feasibility of more multi-cycle electricity generation of NTRB-rGO/CF. For the single-batch discharge experiment in Fig. 6b, the applied load was 20 Ω. The discharge was stopped when the voltage dropped to 10 mV. The single-batch discharge time of the NTRB-rGO/CF was 1.9 h. The battery voltage decreased at a slow rate between 0 and 0.8 h. After 0.8 h, the battery voltage showed a rapid decrease, which was attributed to the decrease in the concentration of active substances in the cathode due to the continuous depletion of copper ions in the cathode liquid, and the energy density reached 1152.7 Wh/m³. Through theoretical calculations of the low-grade waste heat regeneration process, it was found that the thermal efficiency of the NTRB-rGO/CF obtained was 0.61 %, which is in the liquid-based low-temperature waste heat recovery device was very competitive.

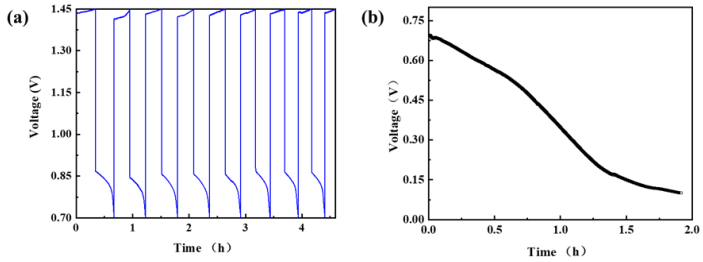


Fig.6 GCD test(a) and the discharge curve (b) of the NTRB-CF/rGO.

## 4 CONCLUSION

To improve the electricity generation of non-aqueous thermally regenerative batteries (NTRBs), The porous carbon foam modified with rGO was prepared using the polyurethane foam template method. The maximum power density of NTRB was increased to 190.2 $W/m^2$. That was mainly due to decreased mass transfer resistance, increased specific surface area, and abundant defects of rGO/CF, thus enhancing the electricity generation of NTRBs. In addition, the feasibility of multi-batch cycle discharge was verified. The energy density of NTRB-rGO/CF in a single batch was 1152.7 $Wh/m^3$, while the thermal efficiency was 0.61%. Furthermore, the excellent stability of rGO/CF was demonstrated throughout the 270-minute power generation cycling. The excellent electricity generation and stable multi-cycle discharge demonstrated a very broad application prospect of NTRB-rGO/CF in low-grade waste heat thermoelectric conversion. In the future application, the application of the NTRB-rGO/CF could be a possible solution for the waste heat energy in the industries. Moreover， the low-grade waste heat(< 80℃) in our social life could also be stored in the NTRB for the evaporation of acetonitrile.

## ACKNOWLEDGMENT

This work was supported by the Foundation for Innovative Research Group Project of the National Natural Science Foundation of China (No. 52021004), the National Natural Science Foundation of China (No. 52376045), Natural Science Foundation of Chongqing, China (CSTB2022NSCQ-MSX1596), Research Project of State Key Laboratory of Engines (K2023-13), and Scientific Research Foundation for Returned Overseas Chinese Scholars of Chongqing, China (No. cx2021088).

## REFERENCE

1. Yuan Z, Wei L, Afroze JD, Goh K, Chen Y, Yu Y, et al. Pressure-retarded membrane distillation for low-grade heat recovery: The critical roles of pressure-induced membrane deformation. J MEMBRANE SCI. 2019;579:90-101.
2. Straub AP, Yip NY, Lin S, Lee J, Elimelech M. Harvesting low-grade heat energy using thermo-osmotic vapour transport through nanoporous membranes. NAT ENERGY. 2016;1:16090.
3. Hur S, Kim S, Kim H, Kumar A, Kwon C, Shin J, et al. Low-grade waste heat recovery scenarios: Pyroelectric, thermomagnetic, and thermogalvanic thermal energy harvesting. NANO ENERGY. 2023;114:108596.
4. Liu Y, Cui M, Ling W, Cheng L, Lei H, Li W, et al. Thermo-electrochemical cells for heat to electricity conversion: from mechanisms, materials, strategies to applications. ENERG ENVIRON SCI. 2022;15:3670-3687.
5. Xu T, Li W, Ma Z, Qian Y, Jiang Q, Luo Y, et al. High power generation from a new semi-solid thermo-electrochemical cell. NANO ENERGY. 2022;103:107826.
6. Qian X, Shin J, Tu Y, Zhang JH, Chen G. Thermally regenerative electrochemically cycled flow batteries with pH neutral electrolytes for harvesting low-grade heat. PHYS CHEM CHEM PHYS. 2021;23:22501-22514.
7. Abdollahipour A, Sayyaadi H. A review of thermally regenerative electrochemical systems for power generation and refrigeration applications. APPL THERM ENG. 2021;187:116576.
8. Wang W, Tian H, Huo D, Shu G. Review of thermally regenerative batteries based on redox reaction and distillation for harvesting low-grade heat as electricity. CHEM ENG J. 2023;474:145503.
9. Shi Y, Zhang L, Zhang Y, Li J, Fu Q, Zhu X, et al. A Self-Stratified Thermally Regenerative Battery Using Nanoprism Cu Covering Ni Electrodes for Low-Grade Waste Heat Recovery. The Journal of Physical Chemistry Letters. 2023;14:1663-1673.
10. Li S, Wang Y, Shi Y, Zhang L, Li J, Zhu X, et al. Nitrogen and Sulfur Co-doped Biomass-Derived Porous Carbon Electrodes for Ultra-High-Performance All-Aqueous Thermally Regenerative Flow Batteries. The Journal of Physical Chemistry Letters. 2024;15:6736-6742.
11. Wang X, Huang Y, Liu C, Mu K, Li KH, Wang S, et al. Direct thermal charging cell for converting low-grade heat to electricity. NAT COMMUN. 2019;10:4151.
12. Mu K, Mu Y, Wang X, Wu X, Pang C, Huang Y, et al. Direct Thermal Charging Cell Using Nickel Hexacyanoferrate (II) Anode for Green Recycling of Low-Grade Heat. ACS ENERGY LETT. 2022;7:1146-1153.
13. Shi Y, Li D, An Y, Zhang L, Li J, Fu Q, et al. Power generation enhancement of a membrane-free thermally regenerative battery induced by the density difference of electrolytes. APPL ENERG. 2023;344.
14. Zhang F, Liu J, Yang WL, Logan BE. A thermally regenerative ammonia-based battery for efficient harvesting of low-grade thermal energy as electrical power. ENERG ENVIRON SCI. 2015;8:343-349.
15. Zhang L, Li YX, Zhu X, Li J, Fu Q, Liao Q, et al. Copper Foam Electrodes for Increased Power Generation in Thermally Regenerative Ammonia-Based Batteries for Low-Grade Waste Heat Recovery. IND ENG CHEM RES. 2019;58:7408-7415.
16. Shi Y, Zhang L, Li J, Fu Q, Zhu X, Liao Q, et al. 3-D printed gradient porous composite electrodes improve anodic current distribution and performance in thermally regenerative flow battery for low-grade waste heat recovery. J POWER SOURCES. 2020;473.
17. Chen PY, Zhang L, Shi Y, Li J, Fu Q, Zhu X, et al. Biomass waste-derived hierarchical porous composite electrodes for high-performance thermally regenerative ammonia-based batteries. J POWER SOURCES. 2022;517.
18. Lu Z, Shi Y, Zhang L, Li Y, Li J, Fu Q, et al. Ammonia crossover in thermally regenerative ammonia-based batteries for low-grade waste heat recovery. J POWER SOURCES.

2022;548.
19. Vicari F, D'Angelo A, Kouko Y, Loffredi A, Galia A, Scialdone O. On the regeneration of thermally regenerative ammonia batteries. J APPL ELECTROCHEM. 2018;48:1381-1388.
20. Maye S, Girault HH, Peljo P. Thermally regenerative copper nanoslurry flow batteries for heat-to-power conversion with low-grade thermal energy. ENERG ENVIRON SCI. 2020;13:2191-2199.
21. Xiao Z, Shi Y, Zhang L, Li J, Fu Q, Zhu X, et al. Performance of a non-aqueous nanofluid thermally regenerative flow battery for electrical energy recovery from low-grade waste heat. APPL THERM ENG. 2024;236:121696.
22. Tang J, Zhao Y, Sunarso J, Wong NH, Zhou J, Zhuo S. Sustainable Polyurethane-Derived Heteroatom-Doped Electrode Materials for Advanced Supercapacitors. CHEMELECTROCHEM. 2022;9:e202200731.
23. Yadav RS, Kuřitka I, Vilcakova J, Skoda D, Urbánek P, Machovsky M, et al. Lightweight NiFe2O4-Reduced Graphene Oxide-Elastomer Nanocomposite flexible sheet for electromagnetic interference shielding application. Composites Part B: Engineering. 2019;166:95-111.
24. Ji Z, Li N, Xie M, Shen X, Dai W, Liu K, et al. High-performance hybrid supercapacitor realized by nitrogen-doped carbon dots modified cobalt sulfide and reduced graphene oxide. ELECTROCHIM ACTA. 2020;334:135632.
25. Shi Y, Zhang L, Li J, Fu Q, Zhu X, Liao Q, et al. Cu/Ni composite electrodes for increased anodic coulombic efficiency and electrode operation time in a thermally regenerative ammonia-based battery for converting low-grade waste heat into electricity. RENEW ENERG. 2020;159:162-171.